

# Unsteady Hydromagnetic Free Convective Flow Past An Infinite Vertical Porous Plate In Porous Medium

Pauline Maina<sup>1\*</sup>, Mathew Kinyanjui<sup>2</sup>, Kang'ethe Giterere<sup>3</sup>

<sup>1, 2 & 3</sup>Department of Pure and Applied Mathematics,

Jomo Kenyatta University of Agriculture and Technology,

P.O. Box 62000- 00200, Nairobi, Kenya.

\*Email of the corresponding author: [pollyweru@gmail.com](mailto:pollyweru@gmail.com)

## ABSTRACT

The effect of heat transfer on unsteady hydromagnetic free convective flow of a viscous incompressible electrically conducting fluid flow past an infinite vertical porous plate in presence of constant injection and heat source has been investigated. The flow is subjected to transverse magnetic field. The partial differential equations governing the flow field has been derived and transformed to non-dimensional form. The equations and their respective initial and boundary conditions are then non-dimensionalized and solved numerically using finite difference method specifically, the Crank-Nicolson method. The effects of varying various flow parameters on the velocity, temperature and concentration profiles have been presented in form of graphs. This has been done when Grashof number for heat transfer,  $Gr_0 > 0$  (cooling of the plate) and also when  $Gr_0 < 0$  (heating of the plate). It has been observed that when the parameters are varied, there is an increase, decrease or no change in velocity, temperature, concentration, skin friction and rate of heat transfer on the surface of the plate. The variation of these parameters especially injection and heat source is very important especially in petroleum engineering where the engineer is able to make various decisions on how to extract fluids as they move through porous medium.

**Key words:** Hydromagnetic, Injection, Porous Medium, Heat Source, Heat transfer

## 1.0 Introduction

Matter can be classified into fluids and solids. A solid can resist shear stress by a static deformation but a fluid cannot. According to McCormack and Crane (1973), a fluid can either be gas or liquid. If the flow variables and fluid properties namely; velocity, pressure, area, density and viscosity do not change with time the flow is said to be steady, otherwise, the flow is unsteady. A fluid is said to be compressible if it changes in volume due to change in pressure whereas it's incompressible if change in density with pressure is so small to be negligible. Hydromagnetic flow occurs when an electrically conducting fluid flows in a magnetic field. Porous medium is a substance that contains pores or voids between solid material through which fluid can pass. In this study, the fluid is taken to be hydromagnetic, incompressible and unsteady. Flows through porous media are very much prevalent in nature and therefore, the study of such flows has become of principal interest in many scientific and engineering applications. These types of flows have shown their great importance in petroleum engineering in the study of movements of natural gas, oil and water through oil reservoirs; in chemical engineering for the filtration and water purification processes. It's also applicable in MHD generators, plasma studies, nuclear reactors, oil exploration, flows in soil, control of pollutant in ground water, coolers, fuel and gas filters, geothermal energy extraction and in the boundary layer control in the field of aerodynamics. Heat transfer in lamina flow is important in problems dealing with chemical reactions and in dissociating fluids.

## 1.1 Literature review

The phenomenon of hydromagnetic flow with heat and mass transfer in an electrically conducting fluid past a porous plate embedded in a porous medium has attracted attention of many investigators because of its varied applications in many engineering problems.

The study of MHD started in the early 1830's with Faraday, who carried out an experiment in which an electrically conducting fluid was passed between poles of magnet in a vacuum glass. Rafael (2005) investigated fluid flow and heat transfer in a porous medium over a stretching surface with internal heat generation and by presence of suction, blowing and impermeability of the surface. He observed that velocity decreases and temperature increases with increasing permeability parameter. He also found that suction decreases velocity while injection increases the velocity. Das *et al.* (2006) estimated the mass transfer effects on unsteady flow past an accelerated vertical porous plate with suction employing finite difference analysis. They observed that porosity parameter retards the velocity of the flow field at all points and also, the higher the suction parameter, the faster the reduction in the velocity of the flow field. Alam *et al.* (2006) studied a steady two dimensional free convection flow and mass transfer past a continuously moving semi-infinite vertical porous plate in a porous

medium. They observed that the temperature decreases with increase in suction parameter and modified Grashof number. Rajeswari *et al.* (2009) studied the effect of chemical reaction on forced and free convection boundary layer that flows in a semi-infinite expanse of an electrically conducting viscous incompressible fluid past vertical porous plate. They observed that in case of uniform magnetic field with suction at the wall of the surface and constant chemical reaction parameter, the velocity of the fluid decreases and the concentration of the fluid increases with increase in suction at the wall of the surface, due to combined effects of the buoyancy force and porosity of the plate. Tamana *et al.* (2009) analyzed heat transfer in a porous medium over a stretching surface with internal heat generation and suction or injection where the study showed that velocity profile decreases with the increase of permeability parameter in both cases of injection or suction. Elbashbeshy *et al.* (2010) studied unsteady boundary layer flow over a porous stretching surface embedded in a porous medium in presence of heat source. He observed that among other things, Nusselt number decreases with increase of porous parameter in the presence of heat source parameter and it also increases with suction. Ferdows *et al.* (2010) analyzed the problem of heat and mass transfer on natural convection adjacent to a vertical plate in a porous medium with high porosity. They observed that the velocity increases when porous parameter increases and the porous parameter has an increasing effect on temperature profiles. Das *et al.* (2011) investigated the mass transfer effects on unsteady hydromagnetic convective flow past a vertical porous plate in a porous medium with heat source, where they found that velocity of the flow field changes more or less with variation of flow parameters.

Chand *et al.* (2012) analyzed an oscillatory hydromagnetic flow through a porous medium bounded by two vertical parallel porous plates where one plate of the channel is kept stationary and the other is moving with uniform velocity. He concluded among other things that the heat transfer is reduced with heat generation parameter and the rate of mass transfer is less for the fluid with large viscosity. Anand *et al.* (2012) analyzed the chemical reaction effects on an unsteady MHD free convection fluid flow past a semi-infinite vertical plate embedded in a porous medium with heat absorption. They observed that the velocity decreases with an increase in the magnetic parameter and it also increases with an increase in the permeability of the porous medium parameter. Ashraf and Hassanin (2013) studied MHD flow past a vertical porous plate through a porous medium under oscillatory suction. They concluded that the magnetic field parameter slows down the velocity of the flow field at all points due to magnetic pull of the Lorentz force acting on the flow field. Sarada and Shanker (2013) studied the effects of Soret and Dufour on unsteady MHD free convection flow past a vertical porous plate in the presence of suction or injection where they observed among other things that suction or injection parameter retards the velocity of flow field at all points.

From the foregoing studies MHD flows on porous medium is an area of interest to many researchers. In this study, an analysis of effects of heat transfer on unsteady MHD free convective flow past a vertical porous plate in a porous medium with heat source and constant injection has been studied numerically.

## 2.1 Mathematical Formulations

Consider the two dimensional flow of a viscous incompressible electrically conducting fluid past an infinite vertical porous plate through a porous medium in presence of uniform transverse magnetic field  $B_0$ , constant heat source ( $Q$ ) and injection ( $V_w$ ). The vertical plate is taken to be the  $x$ -axis and  $y$ -axis normal to it. All the governing equations will therefore be independent of  $x$ -axis because it is infinite. The fluid motion is two dimensional. The physical sketch and geometry of the problem is shown in figure 1.

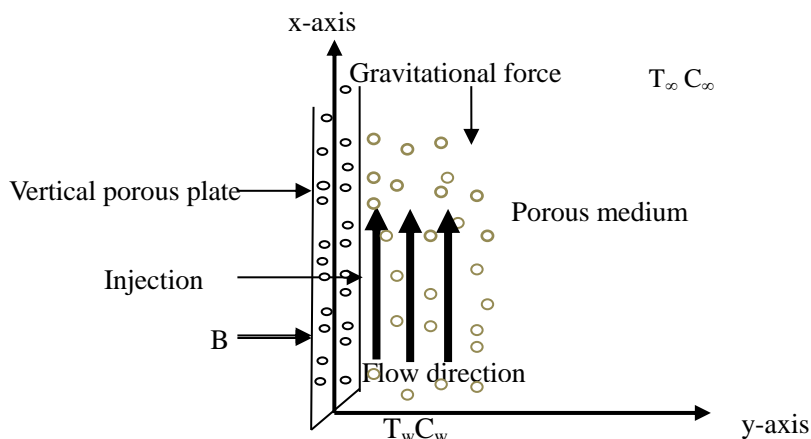


**Figure 1: The Flow Configuration\**

The surface of the vertical plate is at uniform temperature  $T_w$  and concentration  $C_w$ . The temperature and concentration far away from the plate are  $T_\infty$  and  $C_\infty$  respectively. A magnetic field of strength  $B_0$  acts normal to

the plate, i.e. along the y-axis. The density has been assumed to be a linear function of the temperature and species concentration, and therefore the Boussinesq approximation has been used.

### 2.1.1 Continuity equation

In fluid dynamics, the continuity equation is a mathematical statement that, in any steady state process, the rate at which mass enters a system is equal to the rate at which mass leaves the system and is based on the principle of conservation of mass. The differential form of the continuity equation is:

$$\frac{\partial \rho}{\partial t} + \nabla \cdot (\rho \mathbf{u}) = 0 \dots \dots \dots (1a)$$

where  $\rho$  is fluid density,  $t$  is time, and  $\mathbf{u}$  is fluid velocity.

For the case of incompressible flow  $\rho$  is constant and the mass continuity equation simplifies to:

$$\nabla \cdot \mathbf{u} = 0 \dots \dots \dots (1)$$

### 2.1.2 Momentum equations

This is derived from Newton's second law of motion which states that the sum of resultant forces is equal to rate of change of momentum of the flow. The momentum equation in tensor form is written as:

$$\frac{\partial u_i}{\partial t} + v_j \frac{\partial u_i}{\partial y} = -\frac{1}{\rho} \frac{\partial P_i}{\partial x} + \nu \nabla^2 u_i + F_i \dots \dots \dots (2a)$$

Considering the boundary layer approximations, the flow, heat and mass transfer of a fluid in porous medium with Darcian effects and applying the Boussinesq's approximation, the X and Y momentum equations governing the flow in this study will appear as follows:

$$\frac{\partial u}{\partial t} + v \frac{\partial u}{\partial y} = \nu \frac{\partial^2 u}{\partial y^2} - \frac{\nu}{k} u - \frac{\sigma B_0^2}{\rho} u + g\beta(T - T_\infty) + g\beta^*(C - C_\infty) \dots \dots \dots (2)$$

$$\frac{\partial v}{\partial t} + u \frac{\partial v}{\partial y} = \nu \frac{\partial^2 v}{\partial y^2} - \frac{\nu}{k} v - \frac{\sigma B_0^2}{\rho} v + g\beta(T - T_\infty) + g\beta^*(C - C_\infty) \dots \dots \dots (3)$$

### 2.1.3 Equation of energy

The equation of energy is derived from the first law of Thermodynamics, which states that energy is conserved in any process involving a thermodynamic system and its surroundings.

Considering flow of an incompressible fluid with constant thermal conductivity  $k$ , thermal energy equation is expressed as

$$\rho c_p \frac{DT}{Dt} = \nabla \cdot (k \nabla T) + \mu \left( \frac{\partial u_i}{\partial x_j} + \frac{\partial u_j}{\partial x_i} \right)^2 \dots \dots \dots (4a)$$

Considering the boundary layer approximations, the flow, heat and mass transfer of a fluid in porous medium with Darcian effects, injection, heat source and neglecting the induced magnetic field and Joule heat dissipation and applying the Boussinesq's approximation, the energy equation governing the flow in this study will be given as follows:

$$\frac{\partial T}{\partial t} + v \frac{\partial T}{\partial y} = \frac{k}{C_p} \frac{\partial^2 T}{\partial y^2} + \frac{\nu}{C_p} \left( \frac{\partial u}{\partial y} \right)^2 + Q(T - T_\infty) \dots \dots \dots (4)$$

### 2.1.4 The equation for species concentration

The equation of species concentration is based on the conservation of mass. It is applicable when the porous medium is saturated with fluid and when Darcy law is applicable. It is given as follows:

$$\frac{\partial C}{\partial t} + v \frac{\partial C}{\partial y} = D_M \frac{\partial^2 C}{\partial y^2} \dots \dots \dots (5)$$

The boundary and initial conditions are as follows:

At  $y=0$ :  $u=0$ ,  $v=v_w$ ,  $T=T_w$ ,  $C=C_w$

As  $y \rightarrow \infty$ ,  $u \rightarrow 0$ ,  $T \rightarrow T_\infty$ ,  $C \rightarrow C_\infty$

At  $t=0$ ,  $u=u_\infty$ ,  $v=v_w$ ,  $T=T_\infty$ ,  $C=C_\infty$

To non-dimensionalize equations (2), (3), (4) and (5) and their respective boundary conditions the following non-dimensional parameters and variables defined as given below have been used:

$$y^* = \frac{y U_\infty}{\nu}, \quad t^* = \frac{t U_\infty^2}{\nu}, \quad v^* = \frac{v}{U_\infty}, \quad u^* = \frac{u}{U_\infty}, \quad T^* = \frac{T - T_\infty}{T_w - T_\infty}, \quad C^* = \frac{C - C_\infty}{C_w - C_\infty}$$

### 2.1.5 Governing equations in non-dimensional form

$$\frac{\partial u^*}{\partial t^*} + v^* \frac{\partial u^*}{\partial y^*} = \frac{\partial^2 u^*}{\partial y^{*2}} - \left( M + \frac{1}{K_p} \right) u^* + Gr_0 T^* + Gr_c C^* \dots\dots\dots(6)$$

$$\frac{\partial v^*}{\partial t^*} + u^* \frac{\partial v^*}{\partial y^*} = \frac{\partial^2 v^*}{\partial y^{*2}} - \left( M + \frac{1}{K_p} \right) v^* + Gr_0 T^* + Gr_c C^* \dots\dots\dots(7)$$

$$\frac{\partial T^*}{\partial t^*} + v^* \frac{\partial T^*}{\partial y^*} = \frac{1}{Pr} \frac{\partial^2 T^*}{\partial y^{*2}} + Ec \left( \frac{\partial u^*}{\partial y^*} \right)^2 + Q^* T^* \dots\dots\dots(8)$$

$$\frac{\partial C^*}{\partial t^*} + v^* \frac{\partial C^*}{\partial y^*} = \frac{1}{Sc} \frac{\partial^2 C^*}{\partial y^{*2}} \dots\dots\dots(9)$$

where

$$M = \frac{\sigma B_0^2 v}{\rho U_\infty^2}, \quad K_p = \frac{U_\infty^2 k}{v^2}, \quad Ec = \frac{U_\infty^2}{C_p (T_w - T_\infty)}, \quad Q^* = \frac{Qv}{U_\infty^2}, \quad Pr = \frac{v C_p}{K}$$

$$Gr_0 = \frac{v g \beta (T_w - T_\infty)}{U_\infty^3}, \quad Gr_c = \frac{v g \beta^* (C_w - C_\infty)}{U_\infty^3}, \quad Sc = \frac{v}{D_M}$$

The boundary conditions for equations (2), (3), (4) and (5) in non-dimensional form are:

$$\text{At } y^* = 0, \quad u^* = 0, \quad v^* = \frac{v_w}{U_\infty}, \quad T^* = 1, \quad C^* = 1,$$

$$\text{As } y^* \rightarrow \infty, \quad u^* \rightarrow 0, \quad T^* \rightarrow 0, \quad C^* \rightarrow 0,$$

$$\text{At } t^* = 0, \quad u^* = 1, \quad v^* = \frac{v_w}{U_\infty}, \quad T^* = 0, \quad C^* = 0$$

## 2.2 Method of solution

The equations 6, 7, 8 and 9 are solved numerically using the FDM that applies Crank-Nicolson algorithm. To provide this accuracy, difference approximations are developed at the midpoint of the time increment.

### 2.2.1 Equation of momentum:

$$\frac{U_j^{i+1} - U_j^i}{\Delta t} + V_j^i \frac{U_j^{i+1} - U_{j-1}^{i+1} + U_j^i - U_{j-1}^i}{2\Delta y} = \frac{U_{j-1}^{i+1} - 2U_j^{i+1} + U_{j+1}^{i+1} + U_{j-1}^i - 2U_j^i + U_{j+1}^i}{2(\Delta y)^2}$$

$$- \left( M + \frac{1}{K_p} \right) \left( \frac{U_j^{i+1} + U_j^i}{2} \right) + Gr_0 \left( \frac{T_j^{i+1} + T_j^i}{2} \right) + Gr_c \left( \frac{C_j^{i+1} + C_j^i}{2} \right)$$

making  $U_j^{i+1}$  and  $V_j^{i+1}$  the subject of the formula the equations of momentum along x and y axis becomes;

$$U_j^{i+1} = \left[ U_j^i - \frac{\Delta t}{2\Delta y} V_j^i (-U_{j-1}^{i+1} + U_j^i - U_{j-1}^i) + \frac{\Delta t}{2(\Delta y)^2} (U_{j-1}^{i+1} + U_{j+1}^{i+1} + U_{j-1}^i - 2U_j^i + U_{j+1}^i) - \frac{\Delta t}{2} \left( M + \frac{1}{K_p} \right) U_j^i \right.$$

$$\left. + \frac{\Delta t Gr_0}{2} (T_j^{i+1} + T_j^i) + \frac{\Delta t Gr_c}{2} (C_j^{i+1} + C_j^i) \right] \div \left[ 1 + V_j^i \frac{\Delta t}{2\Delta y} + \frac{\Delta t}{(\Delta y)^2} + \frac{\Delta t}{2} \left( M + \frac{1}{K_p} \right) \right] \dots\dots\dots(10)$$

$$V_j^{i+1} = \left[ V_j^i - \frac{\Delta t}{2\Delta y} V_j^i (-V_{j-1}^{i+1} + V_j^i - V_{j-1}^i) + \frac{\Delta t}{2(\Delta y)^2} (V_{j-1}^{i+1} + V_{j+1}^{i+1} + V_{j-1}^i - 2V_j^i + V_{j+1}^i) - \frac{\Delta t}{2} \left( M + \frac{1}{K_p} \right) V_j^i \right.$$

$$\left. + \frac{\Delta t Gr_0}{2} (T_j^{i+1} + T_j^i) + \frac{\Delta t Gr_c}{2} (C_j^{i+1} + C_j^i) \right] \div \left[ 1 + V_j^i \frac{\Delta t}{2\Delta y} + \frac{\Delta t}{(\Delta y)^2} + \frac{\Delta t}{2} \left( M + \frac{1}{K_p} \right) \right] \dots\dots\dots(11)$$

**2.2.2 Equation of energy:**

$$\frac{T_j^{i+1} - T_j^i}{\Delta t} + V_j^i \left( \frac{T_j^{i+1} - T_{j-1}^{i+1} + T_j^i - T_{j-1}^i}{2\Delta y} \right) = \frac{1}{Pr} \left( \frac{T_{j-1}^{i+1} - 2T_j^{i+1} + T_{j+1}^{i+1} + T_{j-1}^i - 2T_j^i + T_{j+1}^i}{2(\Delta y)^2} \right) + Ec \left( \frac{U_j^{i+1} - U_{j-1}^{i+1} + U_j^i - U_{j-1}^i}{2\Delta y} \right)^2 + Q \left( \frac{T_j^{i+1} + T_j^i}{2} \right)$$

making  $T_j^{i+1}$  the subject of the formula;

$$T_j^{i+1} = \left[ T_j^i - V_j^i \frac{\Delta t}{2\Delta y} (-T_{j-1}^{i+1} + T_j^i - T_{j-1}^i) + \frac{\Delta t}{2Pr(\Delta y)^2} (T_{j-1}^{i+1} + T_{j+1}^{i+1} + T_{j-1}^i - 2T_j^i + T_{j+1}^i) + Ec\Delta t \left( \frac{U_j^{i+1} - U_{j-1}^{i+1} + U_j^i - U_{j-1}^i}{2\Delta y} \right)^2 + Q\Delta t \left( \frac{T_j^i}{2} \right) \right] \div \left[ 1 + \frac{V_j^i}{2\Delta y} + \frac{\Delta t}{Pr(\Delta y)^2} - \frac{Q\Delta t}{2} \right] \dots\dots\dots(12)$$

**2.2.3 Equation of concentration:**

$$\frac{C_j^{i+1} - C_j^i}{\Delta t} + v \frac{C_j^{i+1} - C_{j-1}^{i+1} + C_j^i - C_{j-1}^i}{2\Delta y} = \frac{1}{Sc} \left( \frac{C_{j-1}^{i+1} - 2C_j^{i+1} + C_{j+1}^{i+1} + C_{j-1}^i - 2C_j^i + C_{j+1}^i}{2(\Delta y)^2} \right)$$

making  $C_j^{i+1}$  the subject of the formula;

$$C_j^{i+1} = \left[ C_j^i - v \frac{\Delta t}{2\Delta y} (-C_{j-1}^{i+1} + C_j^i - C_{j-1}^i) + \frac{\Delta t}{2Sc(\Delta y)^2} (C_{j-1}^{i+1} + C_{j+1}^{i+1} + C_{j-1}^i - 2C_j^i + C_{j+1}^i) \right] \div \left[ 1 + v \frac{\Delta t}{2\Delta y} + \frac{\Delta t}{(\Delta y)^2} \right] \dots\dots\dots(13)$$

Equations 10,11,12 and 13 are then solved using Matlab, a computer program.

**3.1 RESULTS AND DISCUSSION**

The effects of the pertinent parameters on the flow field are analysed and discussed with the help of velocity profiles, temperature profiles, and concentration distribution. During numerical calculations,  $Sc = 0.62$  has been chosen to represent water vapour,  $Pr = 0.71$  to represent air at  $20^{\circ}C$ . The results are analysed when heating and cooling of the plate.

From **figure 3.1**, it is observed that, increase in Hartmann number  $M$ , causes a decrease in the magnitude of the velocity profile. When transverse magnetic field is applied to an electrically conducting fluid, it gives rise to a force called the Lorentz force which acts against the flow if the magnetic field is applied in the normal direction as in the present study. This resistive force has a tendency to slow down the motion of the fluid in the boundary layer. It's also observed that an increase in Grashof number for mass transfer ( $Gr_c$ ) causes velocity to decrease.  $Gr_c$  defines the ratio of the species buoyancy force to the viscous hydrodynamic force. Hence its increase implies a reduction in viscous hydrodynamic force.

From **figure 3.2**, it has been observed that an increase in permeability parameter  $K_p$ , accelerates the velocity. In this study, permeability parameter is directly proportional to the actual permeability  $k$  of the porous medium. Hence, increasing  $K_p$  decreases the resistance of the porous medium since permeability physically becomes more with an increase in  $K_p$ . This accelerates the flow and increases the magnitude of the velocity. It has also been observed that an increase in the magnitude of injection parameter ( $V_w$ ) accelerates the velocity of the flow. This is because injection accelerates the velocity of a fluid.

From **figure 3.3**, it shows that increase in Hartmann number  $M$ , causes a decrease in the magnitude of the velocity profile. This is due to Lorentz force which acts against the flow hence decelerating the motion of the fluid. This observation agrees with that of Anand *et al* (2012). It has also been observed that an increase in permeability parameter  $K_p$ , accelerates the velocity. This observation agrees with that of Tamana *et al.* (2009).

From **figure 3.4**, an increase in the magnitude of injection parameter ( $V_w$ ) is found to accelerate the velocity of

the flow. This is because injection accelerates the velocity of a fluid. This observation agrees with Rafael (2005). An increase in Grashof number for mass transfer ( $Gr_c$ ) causes velocity to decrease.  $Gr_c$  defines the ratio of the species buoyancy force to the viscous hydrodynamic force. Hence its increase implies a reduction in viscous hydrodynamic force.

From **figure 3.5** it has been observed that an increase in the injection parameter makes the temperature of the flow to decrease. Injecting fluid particles destabilizes the temperature at the boundary layer. Also, as Eckert number ( $Ec$ ) increases, temperature of the flow increases. This is because  $Ec$  expresses the relationship between the kinetic energy in the flow and the enthalpy. It embodies the conversion of kinetic energy into internal energy by work done against the viscous fluid stresses. The positive Eckert number implies cooling of the plate i.e., loss of heat from the plate to the fluid. Hence, greater viscous dissipative heat causes a rise in the temperature.

From **figure 3.6**, as heat source parameter ( $Q$ ) increases, the temperature of the flow increases at all points. Increase in heat source produces a heating effect hence increase in the temperature. The temperature profiles are found to agree closely with those of Das (2009) and Das et al (2011).

From **figure 3.7** it's observed that an increase in magnitude of the injection parameter leads to an increase in the concentration profile. This is so because injection destabilizes the flow of the fluid. It is also observed that an increase in Schmidt number ( $Sc$ ) decreases the concentration boundary layer thickness of the flow field at all points.

From **figure 3.8** it's observed that concentration field due to variation in Schmidt number ( $Sc$ ) for the gases; hydrogen ( $Sc=0.22$ ), water vapour ( $Sc=0.62$ ) and ammonia ( $Sc=0.78$ ). The concentration distribution is vastly affected by the presence of foreign species ( $Sc$ ) in the flow field. The concentration distribution is found to decrease faster as the diffusing foreign species becomes heavier. Thus higher  $Sc$  leads to a faster decrease in concentration of the flow field, an observation which agrees with that of Reddy *et al* (2013). Also an increase in the injection parameter leads to an increase in the concentration profile.

The values of skin friction and rate of heat transfer (Nusselt number,  $Nu$ ) at the wall are found to be affected by most of the parameters as illustrated in tables 3.1 and 3.2. Table 3.1 illustrates  $Gr_0 > 0$  to represent cooling of the plate i.e. heating of the fluid and in table 3.2,  $Gr_0 < 0$  to represent heating of the plate i.e. cooling of the fluid.

From the **table 3.1** the following observations are made: An increase in Hartmann number ( $M$ ) increases the skin friction at the wall. This is due to Lorentz force which has a tendency of slowing down the motion of the fluid in the boundary layer. Increase in  $M$  also reduces the rate of heat transfer. This is due to an increase in thickness of thermal boundary layer. An increase in Grashof number  $Gr_c$  for mass transfer increases the skin friction and decreases the rate of heat transfer.  $Gr_c$  is the ratio of the species buoyancy force to the viscous hydrodynamic force. Increase in  $Gr_c$  implies reduced viscous hydrodynamic forces that cause decrease in viscous dissipation. This translates to a decrease in the rate of heat transfer. An increase in injection Parameter ( $V_w$ ) has an effect making skin friction to drop and rate of heat transfer to increase. Increase in  $V_w$  reduces the growth of the thermal boundary layer leading to an increased  $Nu$ . An increase in Eckert number ( $Ec$ ) causes the skin friction to increase and Nusselt number ( $Nu$ ) to drop. Increase in  $Ec$  translates to a lower value of temperature difference hence, to a reduced rate of heat transfer. Increase in  $Ec$  leads to an increase in velocity of a fluid hence increase in magnitude of skin friction. An increase in permeability parameter ( $K_p$ ) causes the skin friction to drop and the rate of heat transfer to increase. In this study, permeability parameter is directly proportional to the actual permeability  $k$  of the porous medium. Therefore, increase in  $K_p$  leads to thinner temperature boundary layer, hence increase in the rate of heat transfer. Increase in Schmidt number ( $Sc$ ) causes the skin friction to increase and the rate of heat transfer to decrease.  $Sc$  embodies the ratio of momentum to the mass diffusivity. Physically it relates the relative thickness of the hydrodynamic layer and mass diffusivity. A larger value of  $Sc$  means presence of a heavier fluid hence as it increases, the rate of heat transfer will decrease and skin friction to increase. An increase in heat source parameter ( $Q$ ) leads to an increase in the skin friction and Nusselt number ( $Nu$ ) to drop. This is because increase in heat source enhances convection currents on the surface of the plate leading to increase in the skin friction. As  $Q$  increases, thermal boundary layer thickens hence temperature difference lowers, leading to a drop in the rate of heat transfer.

An increase in Prandtl number ( $Pr$ ) causes the skin friction to increase and Nusselt number ( $Nu$ ) to drop. This is because Prandtl number is the ratio of viscous force to thermal force. Therefore the viscous force will increase holding the thermal force constant thus increasing the shear stress. An increase in  $Pr$  causes  $Nu$  to drop because smaller value of  $Pr$  is equivalent to an increase in the thermal conductivity of the fluid, and heat is able to diffuse away from the heated surface more rapidly for higher values of  $Pr$ . Hence in the case of smaller Prandtl numbers, the thermal boundary layer is thicker, and the rate of heat transfer is reduced.

From **table 3.2**, the following observations are made: An increase in Grashof number  $Gr_c$  for mass transfer



increases the skin friction and decreases the rate of heat transfer.  $Gr_c$  is the ratio of the species buoyancy force to the viscous hydrodynamic force. Increase in  $Gr_c$  implies reduced viscous hydrodynamic forces that cause decrease in viscous dissipation. This translates to a decrease in the rate of heat transfer. An increase in Eckert number ( $Ec$ ) causes the skin friction to decrease and the Nusselt number ( $Nu$ ) to drop. This is because Eckert number represents conversion of kinetic energy into internal energy by work that is done against the viscous fluid stresses. When the fluid is heated, it becomes less viscous and hence less stress. A positive Eckert number implies cooling of the plate i.e. loss of heat from the plate to the fluid. Increase in  $Ec$  translates to a lower value of temperature difference. Hence, as it increases the rate of heat transfer will drop. Increase in Schmidt number ( $Sc$ ) causes the skin friction to increase and the rate of heat transfer to decrease.  $Sc$  embodies the ratio of momentum to the mass diffusivity. Physically it relates the relative thickness of the hydrodynamic layer and mass diffusivity. A larger value of  $Sc$  means presence of a heavier fluid hence increase in skin friction, and decrease in the rate of heat transfer. An increase in Prandtl number ( $Pr$ ) causes the skin friction to decrease. An increase in  $Pr$  causes  $Nu$  to drop because smaller value of  $Pr$  is equivalent to an increase in the thermal conductivity of the fluid, and heat is able to diffuse away from the heated surface more rapidly for higher values of  $Pr$ . Hence in the case of smaller Prandtl numbers, the thermal boundary layer is thicker, and the rate of heat transfer is reduced. As permeability parameter ( $K_p$ ) increases, the rate of heat transfer increases and skin friction decreases. This observation is due to the fact that increase in  $K_p$  leads to thinner temperature boundary layer, hence increase in the rate of heat transfer. Increasing  $K_p$  decreases the resistance of the porous medium since permeability physically increases with an increase in  $K_p$  hence a drop in skin friction. An increase in magnitude of injection parameter ( $V_w$ ) causes the  $Nu$  to increase and skin friction to decrease. This is because  $V_w$  destabilizes the flow causing the rate of heat transfer to increase. Thermal boundary layer thickness decreases with increase in injection, leading to an increase in the rate of heat transfer. An increase in heat source parameter ( $Q$ ) causes the  $Nu$  to drop and decrease in skin friction. Thermal boundary layer thickens leading to lower rate of heat transfer. Since in this case there is heating of the fluid, hence when  $Q$  increases, velocity lowers leading to a decrease in skin friction. Increase in Hartmann number ( $M$ ) reduces the rate of heat transfer due to the magnetic pull of the Lorentz force acting on the flow field which has a tendency of slowing down the motion of the fluid in the boundary layer. Increase in  $M$  also reduces the rate of heat transfer due to an increase in thickness of thermal boundary layer.

These observations agree closely with those of Das *et al* (2011).

## CONCLUSION

The objective of this study was to determine the effects of flow variables on unsteady hydromagnetic free convective flow of a viscous incompressible electrically conducting fluid past an infinite vertical porous plate in presence of constant injection and heat source. It has been observed that, increasing injection parameter accelerates the velocity of the flow field, increases the concentration and reduces the temperature of the flow field. It also increases the skin friction at the wall and decreases the rate of heat transfer. A growing Hartmann number ( $M$ ) retards the velocity of the fluid, increases the skin friction at the wall and reduces the rate of heat transfer. Increase in heat source parameter increases the temperature of the flow field, skin friction at the wall and reduces the rate of heat transfer. A growing permeability parameter accelerates the velocity and decreases the temperature of the flow field when  $Gr_0 > 0$  and reverses when  $Gr_0 < 0$ . It also reduces the skin friction and increases the rate of heat transfer at the wall. Increase in Schmidt number has an effect of reducing the concentration of the flow field. It also increases the skin friction at the wall and the rate of heat transfer decreases.

The present work can provide basis for further research by considering; flow that involves non-Newtonian fluids, flow subjected to variable magnetic field, flow with variable injection or suction, flow subjected to variable heat source, flow with Hall and ion-slip currents or three dimensional flow.

## REFERENCES

- Alam M. S., Ferdows M., Ota M. and Maleque M.A., (2006), Dufour and sores effects on unsteady free convection and mass transfer flow past a semi-infinite vertical porous plate in a porous medium, *International Journal of Applied Mechanics and Engineering*, **11**(3): 535-545.
- Anand J., Sivaiah S. and Srinivasa R., (2012), Chemical reaction effects on an unsteady MHD free convection fluid flow past a semi-infinite vertical plate embedded in a porous medium with heat absorption, *Journal of Applied Fluid Mechanics*, **5** (3): 63-70.
- Ashraf A. M. and Hassanin W. S., (2013), Solution of MHD flow past a vertical porous plate through a porous medium under oscillatory suction, *Applied Mathematics*, **4**: 694-702.

Chand K., Kumar R. and Sharma S., (2012), Hydromagnetic oscillatory flow through a porous medium bounded by two vertical porous plates with heat source and sores effect, *Advances in Applied science Research*, **3** (4): 2169-2178.

Das S.S., Sahoo S.K. and Dash G.C., (2006), Numerical solution of mass transfer effects on unsteady flow past an accelerated vertical porous plate with suction, *Bulletin of the Malaysian Mathematical Sciences Society*, **29**(1): 33-42.

Das S.S., Biswal S.R., Tripathy U.K. and Das P., (2011), Mass transfer effects on unsteady hydromagnetic convective flow past a vertical porous plate in a porous medium with heat source, *Journal of Applied Fluid Mechanics*, **4**(4): 91-100.

Elbasheshy E. M.A., Yassmin D.M and Dalia A.A., (2010), Heat transfer over an unsteady porous stretching surface embedded in a porous medium with variable heat flux in the presence of heat source or sink, *African Journal of Mathematics and Computer Science research*, **3** (5): 68-73.

Ferdows M., Koji Kaino and Chien-Hsin Chen, (2010), Dufour, sores and viscous dissipation effects on heat and mass transfer in porous media with high porosities, *International Journal of Applied Engineering Research*, **5** (3): 477-484.

McCormack P.D. and Crane L. J (1973), *Physical Fluid Dynamics*, Academic Press, Newyork.

Rafael Cortell, (2005), Flow and heat transfer of a fluid through a porous medium over a stretching surface with internal heat generation/absorption and suction/blowing, *Fluid Dynamics Research*, **37**: 231-245.

Rajeswari R., Jothiram B. and Nelson V.K., (2009), Chemical reaction, heat and mass transfer on nonlinear MHD boundary layer flow through a vertical porous surface in the presence of suction, *Applied mathematical sciences*, **3** (50): 2469-2480.

Sarada K. and B. Shanker, (2013), Effects of sores and dufour on unsteady MHD free convection flow past a vertical porous plate in the presence of suction or injection, *International Journal of Engineering and Science*, **2** (7): 13-25.

Tamana S., Sumon S., Mohammad M.R. and Goutam S., (2009), Heat transfer in a porous medium over a stretching surface with internal heat generation and suction or injection in the presence of radiation, *Journal of Mechanical Engineering*, **40** (1): 22-28.

## NOMENCLATURE

### ROMAN SYMBOLS

**E** Electric intensity vector, [ $Vm^{-1}$ ].  
**F<sub>i</sub>** Body force, [N].  
**e** Unit charge, [C].  
**L** Characteristic length, [m].  
**J** Current density, [ $Am^{-2}$ ].  
**P** Pressure force, [ $Nm^{-2}$ ].  
**P\*** Dimensionless Pressure force.  
**u** Characteristic velocity, [ $ms^{-1}$ ]  
**t** Dimensional time, [s]  
**N** Thermal conductivity, [ $Wm^{-1}k^{-1}$ ].  
**q** Velocity vector, [ $ms^{-1}$ ].  
**B** Magnetic field vector, [ $Wbm^{-2}$ ].  
**D** Electric displacement vector, [ $cm^{-2}$ ].  
**H** Magnetic field intensity vector, [ $Wbm^{-2}$ ].  
**i, j, k** Unit vectors in the x, y, and z directions  
**u, v, w** Components of velocity vector **q**  
**F<sub>e</sub>** Electromagnetic force, [ $kgms^{-2}$ ].  
**Q** Amount of heat added to a system, [Nm].  
**D<sub>M</sub>** Molecular diffusion coefficient, [ $m^2s^{-1}$ ]  
**C<sub>p</sub>** Specific heat at constant pressure, [ $Jkg^{-1}k^{-1}$ ]  
**T** Absolute free temperature of the fluid, [K].  
**T<sub>∞</sub>** Characteristic free stream temperature, [K].  
**u\*, v\*, w\*** Dimensionless fluid velocity  
**V<sub>w</sub>** Injection parameter

**x\*, y\*, z\*** Dimensionless Cartesian coordinates  
**t\*** Dimensionless time  
**u\*** Dimensionless velocity  
**P\*** Dimensionless pressure force  
**Pr** Prandtl number  
**Nu** Nusselt number  
**M** Hartmann parameter  
**Gr<sub>θ</sub>** Grashof number for heat transfer.  
**Gr<sub>c</sub>** Grashof number for mass transfer.

### GREEK SYMBOLS

**μ** Coefficient of viscosity, [ $kgm^{-1}s^{-1}$ ]  
**γ** Kinematic viscosity, [ $m^2s^{-1}$ ]  
**ρ** Fluid density, [ $kgm^{-3}$ ].  
**ρ<sub>e</sub>** Electrical charge density, [ $cm^{-2}$ ].  
**σ** Electrical conductivity, [ $Ω^{-1}m^{-1}$ ].  
**μ<sub>e</sub>** Magnetic permeability, [ $Hm^{-1}$ ].  
**Δx, Δy, Δz** Distance intervals  
**Δt** Time interval  
**ΔT** Temperature change, [K].  
**∇** Gradient operator, [ $i \frac{\partial}{\partial x} + j \frac{\partial}{\partial y} + k \frac{\partial}{\partial z}$ ].  
**φ** Viscous dissipation function, [ $s^2$ ].

### ABBREVIATIONS

**FDM** Finite difference Method  
**ODE** Ordinary differential equations  
**MHD** Magnetohydrodynamic  
**PDE** Partial Differential equations



**Table 3.1:** Values of skin friction ( $\tau$ ) and rate of heat transfer (Nu) at the wall for  $Gr_0 > 0$

| M   | V <sub>w</sub> | Q    | K <sub>p</sub> | Pr    | Ec  | Sc   | Gr <sub>c</sub> | $\tau$           | Nu               |
|-----|----------------|------|----------------|-------|-----|------|-----------------|------------------|------------------|
| 0.5 | -0.1           | 0.01 | 0.5            | 0.71  | 1.0 | 0.62 | 15              | <b>7.480937</b>  | <b>2.210481</b>  |
| 2.5 | -0.1           | 0.01 | 0.5            | 0.71  | 1.0 | 0.62 | 15              | <b>7.907399</b>  | <b>2.062789</b>  |
| 5.0 | -0.1           | 0.01 | 0.5            | 0.71  | 1.0 | 0.62 | 15              | <b>8.412898</b>  | <b>1.882545</b>  |
| 0.5 | 1.0            | 0.01 | 0.5            | 0.71  | 1.0 | 0.62 | 15              | <b>6.480961</b>  | <b>15.239438</b> |
| 0.5 | 2.0            | 0.01 | 0.5            | 0.71  | 1.0 | 0.62 | 15              | <b>5.794819</b>  | <b>17.137171</b> |
| 0.5 | -0.1           | 1.00 | 0.5            | 0.71  | 1.0 | 0.62 | 15              | <b>7.481550</b>  | <b>1.996173</b>  |
| 0.5 | -0.1           | 2.50 | 0.5            | 0.71  | 1.0 | 0.62 | 15              | <b>7.482505</b>  | <b>1.662497</b>  |
| 0.5 | -0.1           | 0.01 | 0.1            | 0.71  | 1.0 | 0.62 | 15              | <b>9.073508</b>  | <b>1.639534</b>  |
| 0.5 | -0.1           | 0.01 | 0.05           | 0.71  | 1.0 | 0.62 | 15              | <b>10.705047</b> | <b>1.010938</b>  |
| 0.5 | -0.1           | 0.01 | 0.5            | 0.015 | 1.0 | 0.62 | 15              | <b>7.467723</b>  | <b>6.743481</b>  |
| 0.5 | -0.1           | 0.01 | 0.5            | 0.64  | 1.0 | 0.62 | 15              | <b>7.479355</b>  | <b>2.757300</b>  |
| 0.5 | -0.1           | 0.01 | 0.5            | 0.71  | 0.4 | 0.62 | 15              | <b>7.478331</b>  | <b>3.089354</b>  |
| 0.5 | -0.1           | 0.01 | 0.5            | 0.71  | 2.0 | 0.62 | 15              | <b>7.485289</b>  | <b>0.742829</b>  |
| 0.5 | -0.1           | 0.01 | 0.5            | 0.71  | 1.0 | 0.22 | 15              | <b>7.489135</b>  | <b>2.206333</b>  |
| 0.5 | -0.1           | 0.01 | 0.5            | 0.71  | 1.0 | 0.78 | 15              | <b>7.478231</b>  | <b>2.211746</b>  |
| 0.5 | -0.1           | 0.01 | 0.5            | 0.71  | 1.0 | 0.62 | -30             | <b>7.334084</b>  | <b>2.262127</b>  |
| 0.5 | -0.1           | 0.01 | 0.5            | 0.71  | 1.0 | 0.62 | 90              | <b>7.725698</b>  | <b>2.122493</b>  |
| 0.5 | -0.1           | 0.01 | 0.5            | 0.71  | 1.0 | 0.62 | 150             | <b>7.921511</b>  | <b>2.050380</b>  |

**Table 3.2:** Values of skin friction ( $\tau$ ) and rate of heat transfer (Nu) at the wall for  $Gr_0 < 0$

| M   | V <sub>w</sub> | Q    | K <sub>p</sub> | Pr    | Ec  | Sc   | Gr <sub>c</sub> | $\tau$          | Nu               |
|-----|----------------|------|----------------|-------|-----|------|-----------------|-----------------|------------------|
| 0.5 | -0.1           | 0.01 | 0.5            | 0.71  | 1.0 | 0.62 | 15              | <b>7.367835</b> | <b>2.251693</b>  |
| 2.5 | -0.1           | 0.01 | 0.5            | 0.71  | 1.0 | 0.62 | 15              | <b>7.707331</b> | <b>2.138159</b>  |
| 5.0 | -0.1           | 0.01 | 0.5            | 0.71  | 1.0 | 0.62 | 15              | <b>8.108252</b> | <b>2.001507</b>  |
| 0.5 | 1.0            | 0.01 | 0.5            | 0.71  | 1.0 | 0.62 | 15              | <b>6.450017</b> | <b>15.241675</b> |
| 0.5 | 2.0            | 0.01 | 0.5            | 0.71  | 1.0 | 0.62 | 15              | <b>5.776377</b> | <b>17.137896</b> |
| 0.5 | -0.1           | 1.00 | 0.5            | 0.71  | 1.0 | 0.62 | 15              | <b>7.367225</b> | <b>2.038474</b>  |
| 0.5 | -0.1           | 2.50 | 0.5            | 0.71  | 1.0 | 0.62 | 15              | <b>7.366275</b> | <b>1.706530</b>  |
| 0.5 | -0.1           | 0.01 | 0.1            | 0.71  | 1.0 | 0.62 | 15              | <b>8.629674</b> | <b>1.820225</b>  |
| 0.5 | -0.1           | 0.01 | 0.05           | 0.71  | 1.0 | 0.62 | 15              | <b>9.904830</b> | <b>1.364597</b>  |
| 0.5 | -0.1           | 0.01 | 0.5            | 0.64  | 1.0 | 0.62 | 15              | <b>7.369399</b> | <b>2.252936</b>  |
| 0.5 | -0.1           | 0.01 | 0.5            | 0.015 | 1.0 | 0.62 | 15              | <b>7.380927</b> | <b>6.743984</b>  |
| 0.5 | -0.1           | 0.01 | 0.5            | 0.71  | 2.0 | 0.62 | 15              | <b>7.363627</b> | <b>0.832242</b>  |
| 0.5 | -0.1           | 0.01 | 0.5            | 0.71  | 0.4 | 0.62 | 15              | <b>7.370365</b> | <b>3.105000</b>  |
| 0.5 | -0.1           | 0.01 | 0.5            | 0.71  | 1.0 | 0.78 | 15              | <b>7.365137</b> | <b>2.252936</b>  |
| 0.5 | -0.1           | 0.01 | 0.5            | 0.71  | 1.0 | 0.22 | 15              | <b>7.376010</b> | <b>2.247620</b>  |
| 0.5 | -0.1           | 0.01 | 0.5            | 0.71  | 1.0 | 0.62 | -30             | <b>7.221291</b> | <b>2.302524</b>  |
| 0.5 | -0.1           | 0.01 | 0.5            | 0.71  | 1.0 | 0.62 | 90              | <b>7.612070</b> | <b>2.165076</b>  |
| 0.5 | -0.1           | 0.01 | 0.5            | 0.71  | 1.0 | 0.62 | 150             | <b>7.807453</b> | <b>2.094073</b>  |

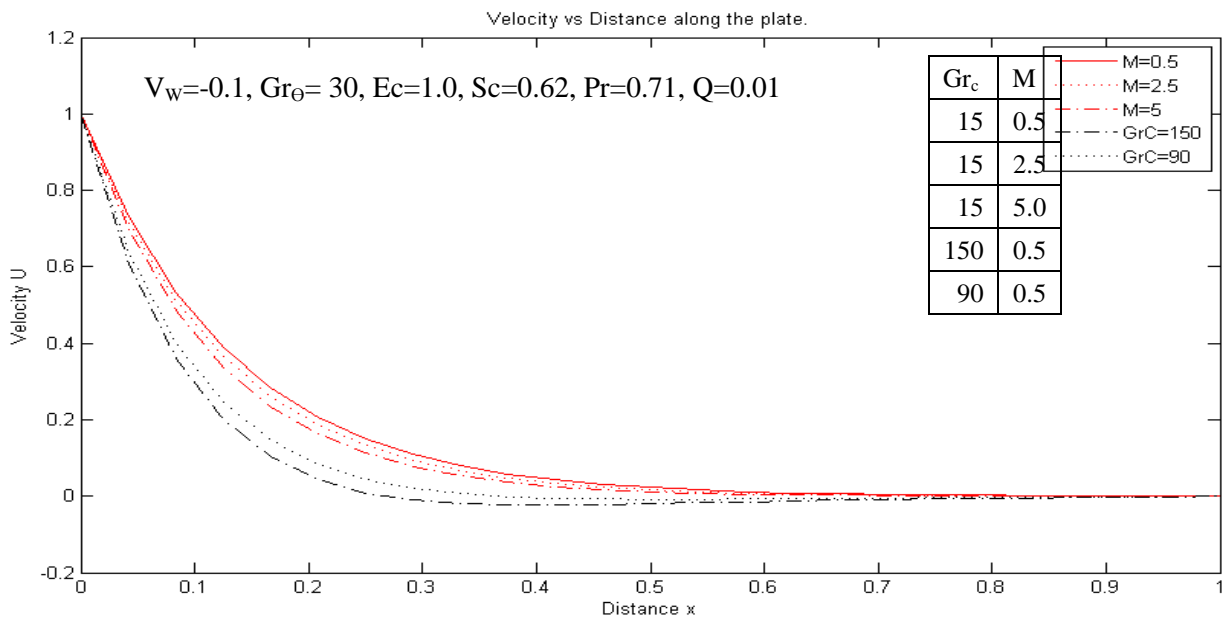


**Fig 3.1: Velocity profile for  $Gr_0 > 0$  with variation of  $M$  and  $Gr_c$**

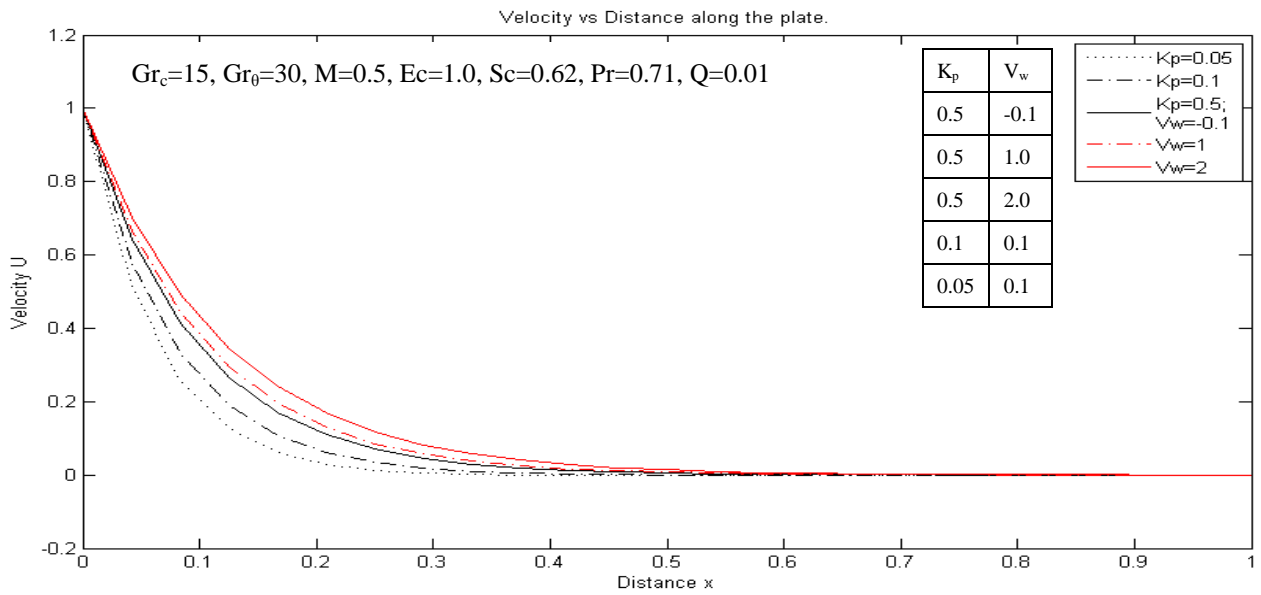


**Fig 3.2: Velocity profile for  $Gr_0 > 0$  with variation of  $V_w$  and  $K_p$**

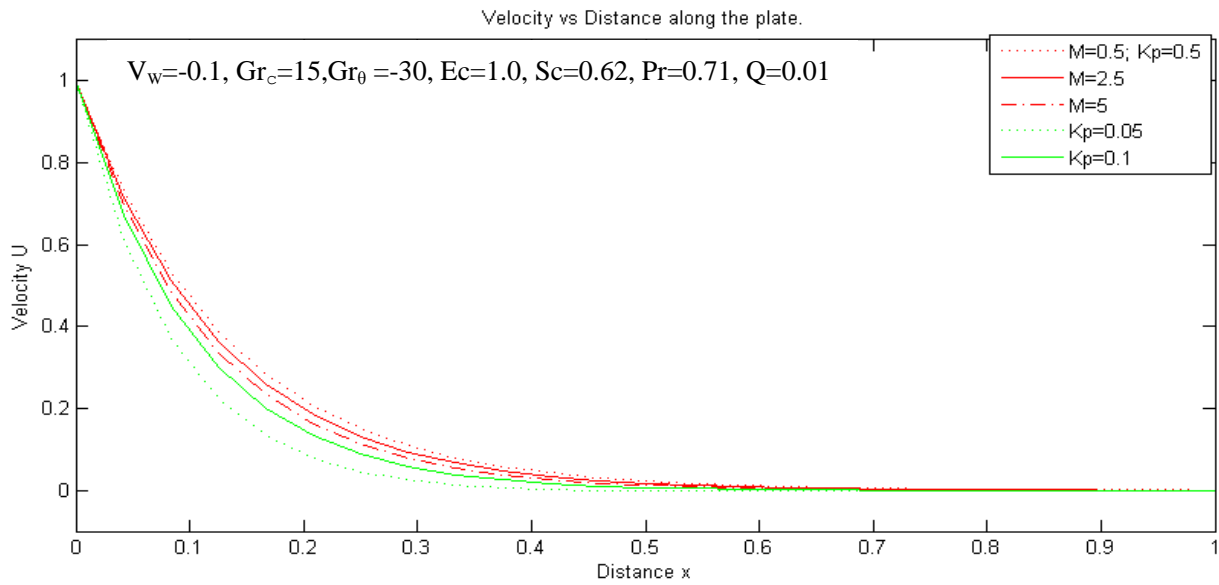


**Fig 3.3: Velocity profile for  $Gr_0 > 0$  with variation of  $M$  and  $K_p$**

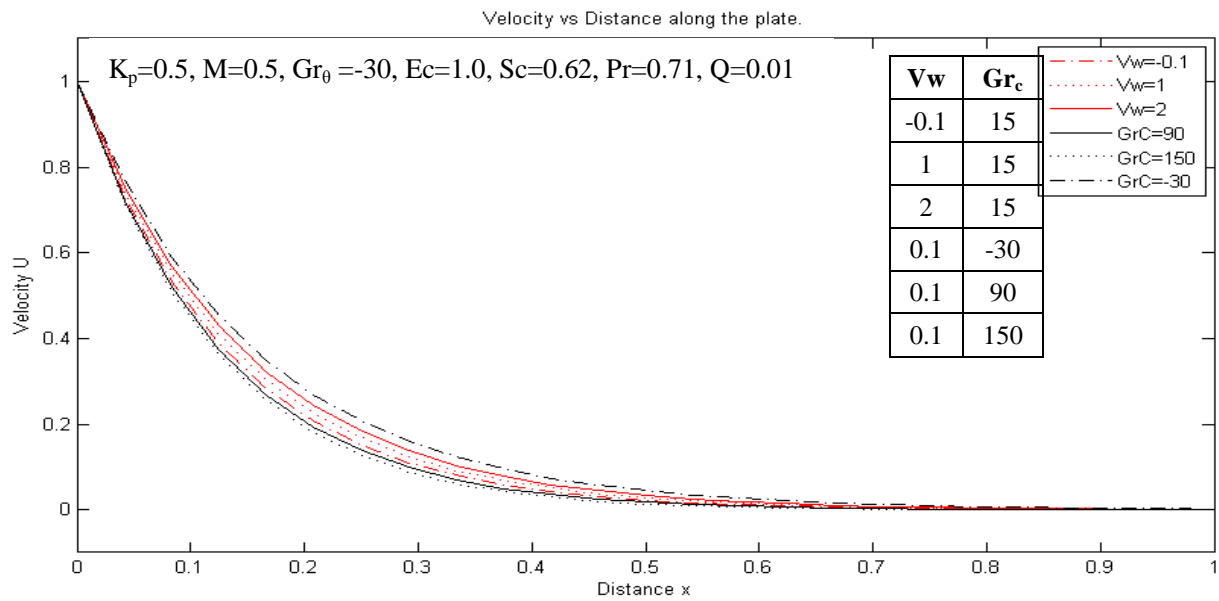


**Fig 3.4: Velocity profile for  $Gr_0 < 0$  with variation of  $V_w$  and  $Gr_c$**

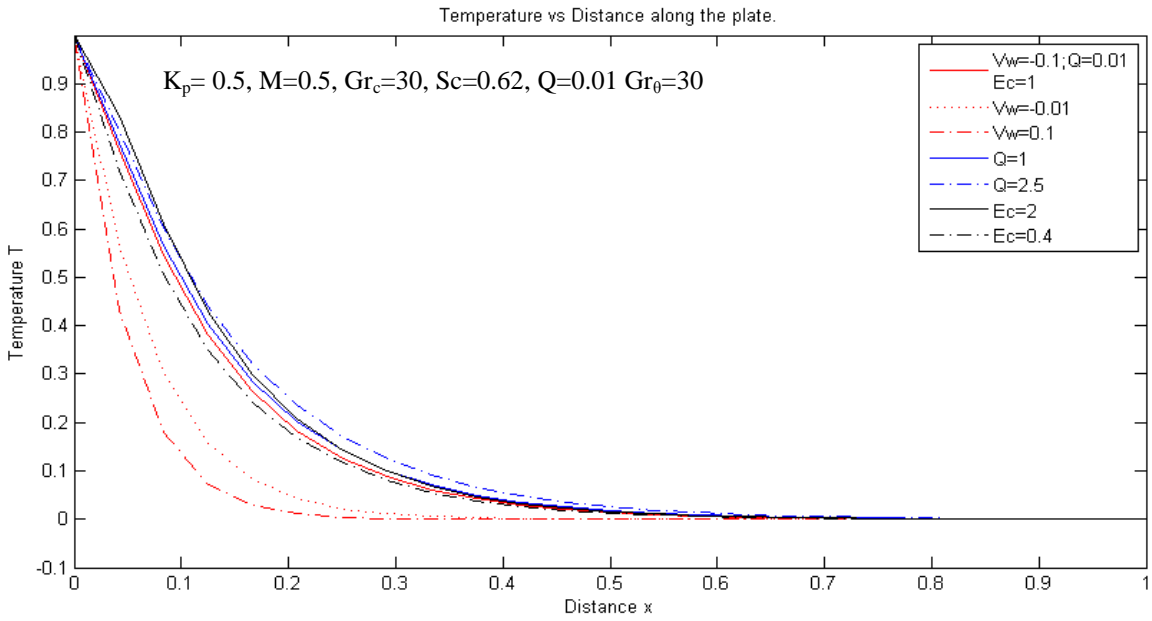


Figure 3.5: Temperature profile for  $Gr_0 > 0$  with variation of  $Q, V_w,$  and  $Ec$

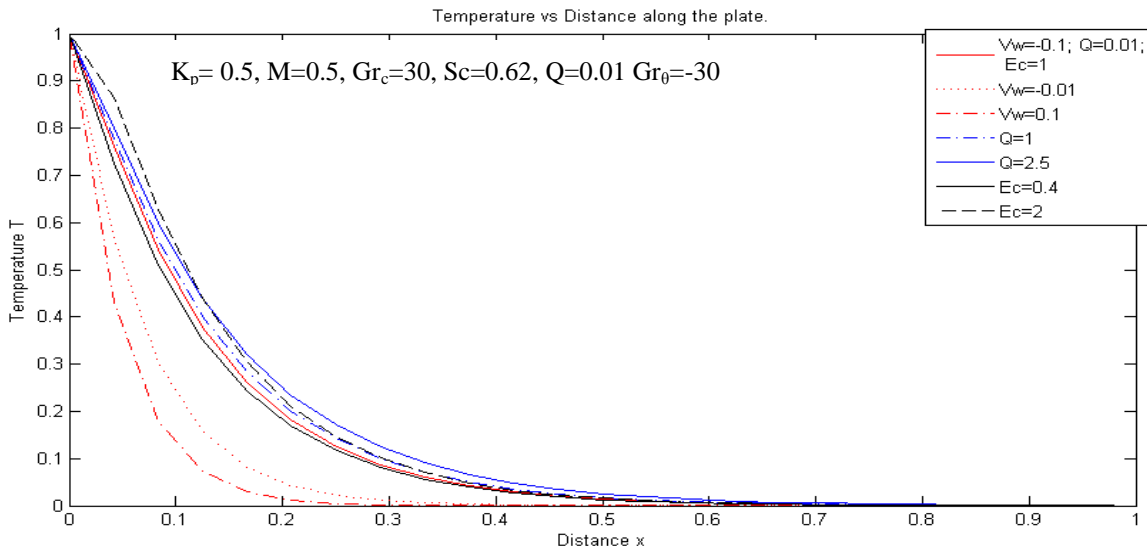
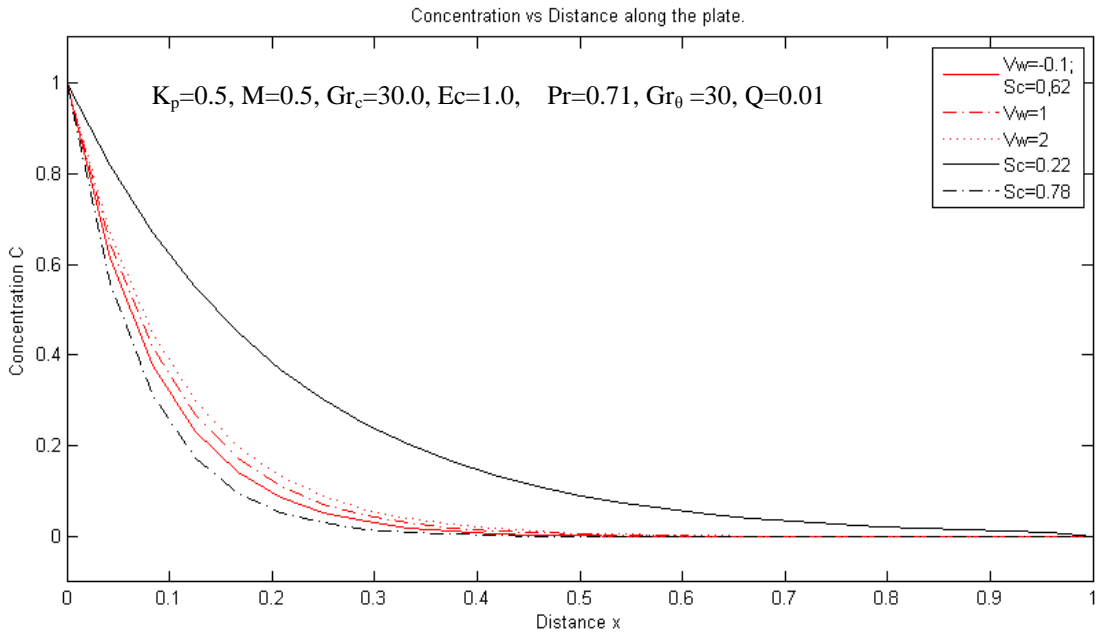
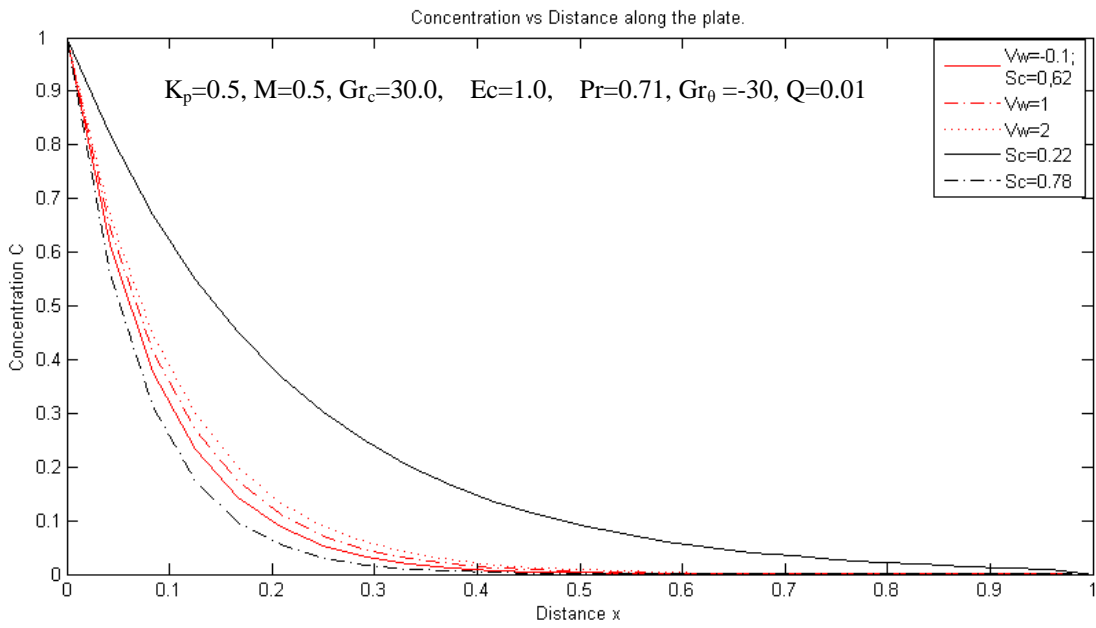


Figure 3.6: Temperature profile for  $Gr_0 < 0$  with variation of  $Q, V_w,$  and  $Ec$



**Figure 3.7: Concentration profile with variation of  $V_w$  and  $Sc$  when  $Gr_0 > 0$**



**Figure 3.8: Concentration profile with variation of  $V_w$  and  $Sc$  when  $Gr_0 < 0$**

The IISTE is a pioneer in the Open-Access hosting service and academic event management. The aim of the firm is Accelerating Global Knowledge Sharing.

More information about the firm can be found on the homepage:

<http://www.iiste.org>

## CALL FOR JOURNAL PAPERS

There are more than 30 peer-reviewed academic journals hosted under the hosting platform.

**Prospective authors of journals can find the submission instruction on the following page:** <http://www.iiste.org/journals/> All the journals articles are available online to the readers all over the world without financial, legal, or technical barriers other than those inseparable from gaining access to the internet itself. Paper version of the journals is also available upon request of readers and authors.

## MORE RESOURCES

Book publication information: <http://www.iiste.org/book/>

Academic conference: <http://www.iiste.org/conference/upcoming-conferences-call-for-paper/>

## IISTE Knowledge Sharing Partners

EBSCO, Index Copernicus, Ulrich's Periodicals Directory, JournalTOCS, PKP Open Archives Harvester, Bielefeld Academic Search Engine, Elektronische Zeitschriftenbibliothek EZB, Open J-Gate, OCLC WorldCat, Universe Digital Library, NewJour, Google Scholar

